Molecular Therapy
Oncology
Original Article

The therapeutic effect of DX2 inhibition in nicotine-induced lung cancer progression

Soyoung Park,[1] Ah-Young Oh,[1] Byung-Su Hong,[1] Yun-Jeong Shin,[2] Hyewon Jang,[2] Hyunghwan Seo,[2] So-mi Kang,[1] Tae-Gyun Woo,[1] Hyo-Pin Park,[1] Jiwon Jeong,[1] Hye-Ju Kim,[1] Bae-Hoon Kim,[1,3] Yonghoon Kwon,[2] and Bum-Joon Park[1]

[1]Department of Molecular Biology, College of Natural Science, Pusan National University, Busan 46241, Republic of Korea; [2]Department of Agricultural Biotechnology, College of Agricultural Science, Seoul National University, Seoul 08826, Republic of Korea; [3]Research Institute of PRG S&Tech, PRG S&Tech Co., Ltd., Busan 46274, Republic of Korea

Alternative splicing products of AIMP2 and AIMP2-DX2 (DX2) have been reported to be associated with human lung cancer. In fact, DX2 expression is elevated in human lung cancers, and DX2 transgenic mice also develop lung cancer, in particular small cell lung cancer (SCLC). However, the mechanism by which DX2 is induced during cancer progression has not been clearly elucidated. Here, we show that DX2 is induced by nicotine, the main component of smoking-related chemicals, which can stabilize the human epidermal growth factor receptor 2 (HER2) protein and transcriptionally increase sonic hedgehog (Shh). Indeed, nicotine showed tumorigenicity via DX2 by promoting spheroid formation and *in vivo* lung and kidney cancer progression. Moreover, the elimination of DX2 using small interfering RNA (siRNA) or an optimized inhibitor (SNU-14) blocked the induction of HER2 and Shh and completely suppressed tumor sphere formation in response to nicotine. These results indicate that DX2 is critical for lung cancer progression, and a specific DX2 inhibitor would be useful for the treatment of human cancers, including SCLC and non-SCLC (NSCLC).

INTRODUCTION

Human lung cancer is the most aggressive malignancy. Worldwide, 1,760,000 patients die of lung cancer, with a very low survival rate.[1] Human lung cancers are divided into two main types, non-small cell lung cancer (NSCLC) and SCLC, based on their histological properties.[2] For SCLC, which occupied 10%–15% of all lung cancers, its molecular pathogenesis is largely unknown due to rapid progression and a lack of surgical specimens. Therefore, proper treatment has not been developed for decades, and the overall survival rate is still only 7%.[3,4] It is also well known that smoking increases lung cancer incidence and is strongly associated with SCLC.[5,6]

In general, human cancer progression is achieved by an initiator and promoter. Initiators contribute to cancer initiation by inducing genetic mutations, so almost all initiators are mutagens.[7] Under smoking conditions, some chemicals, including benzo-(a)-pyrene and smoking tar, have been suggested as mutagens.[8–10] Indeed, the genetic mutation pattern of TP53 in smokers with lung cancer is quite similar to that in non-smokers who have been exposed to smoky coal.[11] These results imply that a similar mutagen, such as benzo-(a)-pyrene, functions as an initiator in lung cancer.

In contrast, a promoter of smoking-related lung cancer has not yet been proposed. In other cancer models such as breast cancer, in which estrogen functions as a promoter, the promoter exhibits a dose-related sigmoidal curve without genetic mutations.[12] Considering that the incidence of SCLC tends to mirror the smoking rate, it may contain a promoter for lung cancer. In addition, smoking habits also increase bladder, kidney, and gastric cancers, indicating that water-soluble and well-circulated chemicals can function as promoters of smoking-related human cancers.[8–10] These features strongly suggest that nicotine is a putative candidate promoter of smoking-related cancers.[13,14]

In our previous study, DX2, an aberrant alternative splicing product of AIMP2, promoted lung cancer progression, in particular SCLC, by inhibiting p14/ARF.[15] DX2 is stabilized by oncogenes such as human epidermal growth factor receptor 2 (HER2)/Neu, AKT, or K-ras and promotes the degradation of p14/ARF. Thus, DX2 inhibitors can induce cell death in lung cancer cell lines and xenograft models. However, we did not reveal how DX2 is induced in the early stages of cancer without oncogenic mutations. Unlike NSCLC, which shows frequent mutation rates in KRAS or ERBB2, SCLC does not show mutations in these oncogenes but mostly shows genetic abnormalities in tumor suppressor genes.[3]

Therefore, we hypothesized that smoking is an important promoter of SCLC and that nicotine and DX2 might be linked to each other. To test this hypothesis, we monitored the effect of nicotine on DX2 expression in SCLC cells and human lung cells. We found that the nicotine-DX2 axis promotes cell proliferation via stabilizing HER2

Received 3 June 2024; accepted 5 September 2024;
https://doi.org/10.1016/j.omton.2024.200875.

Correspondence: Bum-Joon Park, Department of Molecular Biology, College of Natural Science, Pusan National University, Busan 46241, Republic of Korea.
E-mail: bjpark1219@pusan.ac.kr

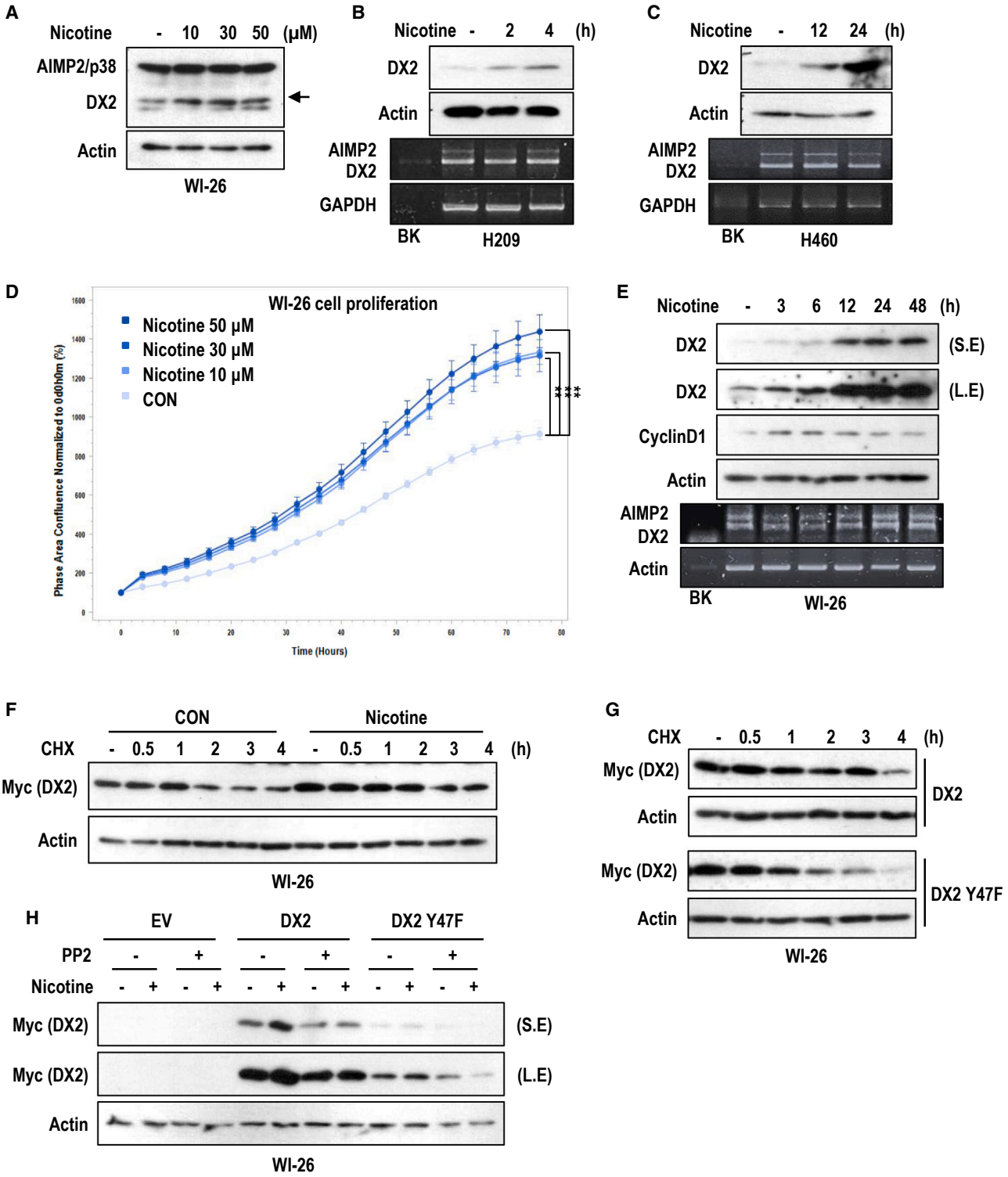

Figure 1. Induction of DX2 expression by nicotine in pulmonary cells

(A) Nicotine induces DX2 expression in a dose-dependent manner in human diploid lung fibroblasts (WI-26). Cells were treated with nicotine at the indicated concentrations for 24 h, and DX2 expression was measured by western blotting. Actin was used as a loading control. (B and C) Nicotine induced DX2 expression only at the protein level. NSCLC (H460) and SCLC (H209) cells were treated with nicotine at 30 μM for the indicated times, and immunoblot or RT-PCR was performed. Actin and GAPDH were used

(legend continued on next page)

in NSCLC and inducing sonic hedgehog (Shh) ligands in SCLC. Notably, nicotine shows tumorigenic abilities in tumor spheroid formation assays and *in vivo*. Therefore, the optimized DX2 inhibitor could be a highly potent drug candidate against smoking-induced cancers.

RESULTS

Nicotine induces DX2 expression

In our previous study, we revealed that DX2 contributes to lung cancer progression, in particular SCLC.[15] Thus, we speculated that nicotine may be related to DX2 expression. To address this, we first checked the expression of DX2 in human pulmonary epithelial-like cells, WI-26. From 10 μM, DX2 expression was increased without AIMP2 alteration (Figure 1A). We also observed the same response in the SCLC cell line H69 (Figure S1A). DX2 induction in response to nicotine was detected in other SCLC cell lines, NCI-H209 (Figure 1B) and NCI-H146 (Figure S1B), as well as NSCLC cells, NCI-H460 (Figure 1C), from 2 to 24 h without transcriptional induction. Since the origin of SCLC has been suggested to be a neuroendocrine cell,[5] we examined the effect of the neuroblastoma cell lines SK-N-MC and SK-N-SH. In both cell lines, nicotine induced DX2 expression without transcriptional induction (Figure S1C) in a time- and dose-dependent manner (Figure S1D). To address the cellular effects of nicotine, we monitored the proliferation of WI-26 cells using a real-time cell counting microscope and found that nicotine promoted cell proliferation (Figure 1D). Consistently, nicotine induced the expression of cyclin D1, a cell cycle inducer (Figure 1E).[16] We also observed an increase in cell viability following nicotine treatment of SK-N-MC (Figure S1E), NCI-H446 (Figure S1F), and 253 J, a human bladder cancer cell line (Figure S1G). Additionally, cyclin D1 induction was detected in NCI-H460 and 253 J cells (Figures S1H and S1I), whereas the elimination of DX2 blocked the induction of cyclin D1 by nicotine (Figure S1J).

Nicotine stabilizes DX2 by phosphorylation

To determine how nicotine induces DX2 expression, we measured the expression of ectopically expressed DX2 and AIMP2. Nicotine treatment increased exogenous DX2 without altering AIMP2 expression (Figure S2A), indicating that nicotine-mediated DX2 increases can be achieved at the post-translational level. Therefore, we monitored the stability of DX2 under nicotine treatment. Nicotine could increase DX2's half-life from 2 to 4 h in WI-26 (Figures 1F and 1G). Similarly, the extension of the DX2 half-life was observed in the SK-N-SH cell system (Figures S2B and S2C). Since nicotine can activate Ca^{2+} signaling,[17,18] we checked the expression of DX2 under BAPTA, a calcium chelator, and found that Ca^{2+} is required for nicotine-induced DX2 stabilization (Figure S2D). Therefore, we searched for a newly generated motif in DX2 by exon 2 skipping and found that the QDY motif was uniquely produced by alternative splicing (Figure S3A). Since the QDY motif is predicted to be phosphorylated by the Src kinase family (Figure S3B), we generated a phosphorylation-defective DX2 mutant (DX2 Y47F). This mutant had a very short half-life (2 h) compared to that of wild-type DX2 (4 h; Figure 1G). In addition, DX2 Y47F levels were not increased by nicotine treatment (Figures 1H and S3C). Moreover, the Src inhibitor PP2 blocked the induction of DX2 by nicotine (Figure 1H). These results suggest that phosphorylation of DX2 by the Src family could increase the protein stability of DX2.

DX2 increases HER2 expression

In our previous study, we showed that nicotine and DX2 promoted cell proliferation (Figure 1D; Govind et al.[14]). To verify the molecular mechanism underlying this effect, we examined the expression of HER2, which is critical for lung cancer progression and cell cycle regulation. In addition, it has been reported that a considerable portion of patients with NSCLC show high HER2 expression without genetic alteration or mRNA induction.[19–21] As expected, nicotine induced HER2 expression in the WI-26 cells (Figure 2A). We confirmed the induction of surface HER2 using fluorescence-activated cell sorting (FACS) analysis (Figure 2B). SK-N-MC cells showed a similar pattern of nicotine-induced total and surface HER2 expression (Figures 2C and 2D) without transcriptional induction (Figures S4A–S4C). Under the same conditions, we observed the induction of DX2 (Figure S4C). Interestingly, the elimination of DX2 completely blocked HER2 induction in response to nicotine and reduced basal HER2 expression (Figure 2E). Considering our previous report that HER2 can increase DX2 expression,[15] there would be a positive feedback loop between HER2 and DX2. Since HER2 can be localized in the nucleus when it is overexpressed,[22,23] we checked HER2 through immunofluorescence (IF). From this experiment, we found that nuclear and surface HER2 was also increased by nicotine (Figures 2F, S4D, and S4E). Additionally, we observed an increase in HER2 stability after nicotine treatment (Figure 2G). Among E3 ligases, Beta-Transducin Repeat Containing E3 Ubiquitin Protein Ligase (β-TrCP) blocked HER2 expression (Figure 2H), and nicotine treatment and DX2 ectopic expression promoted the dissociation of HER2 and β-TrCP (Figures 2I and S4F), which is reported to be responsible for HER2 degradation.[24] Instead, nicotine treatment

for loading. (D) Nicotine induced proliferation of WI-26 cells. Using live-cell imaging analysis, the proliferation of WI-26 cells was measured every 4 h. Error bars indicate the standard deviations (SD). $^{**}p < 0.005$. (E) Nicotine elevated DX2 expression in a time-dependent manner in human diploid lung fibroblasts. Cells were treated with nicotine (30 μM) for the indicated time, and immunoblotting was performed. Actin was used as a loading control. L.E and S.E indicate long exposure and short exposure, respectively. (F) Cycloheximide (CHX) chase assay showed prolonged nicotine-induced DX2 protein stability. After incubation with nicotine at 30 μM for 12 h, cells were treated with CHX for the indicated time. Immunoblotting was performed. Actin was used for the loading. (G) The half-life of DX2 Y47F is shorter than that of wild-type DX2. Myc-tagged vectors encoding wild-type DX2 and DX2 Y47F were transfected into the WI-26 cells. After 24 h, cells were treated for the indicated times. Immunoblot analysis was performed. Actin was used for the loading. (H) Src kinase inhibitor (PP2) blocks nicotine-mediated DX2 induction and does not occur in the DX2 Y47F mutant. Myc-tagged vectors encoding wild-type DX2 and DX2 Y47F were transfected into the WI-26 cells. Subsequently, cells were co-treated with PP2 (10 μM) and nicotine (30 μM) for 12 h. Then immunoblot analysis was performed. Actin was used as a loading control. L.E and S.E indicate long exposure and short exposure, respectively.

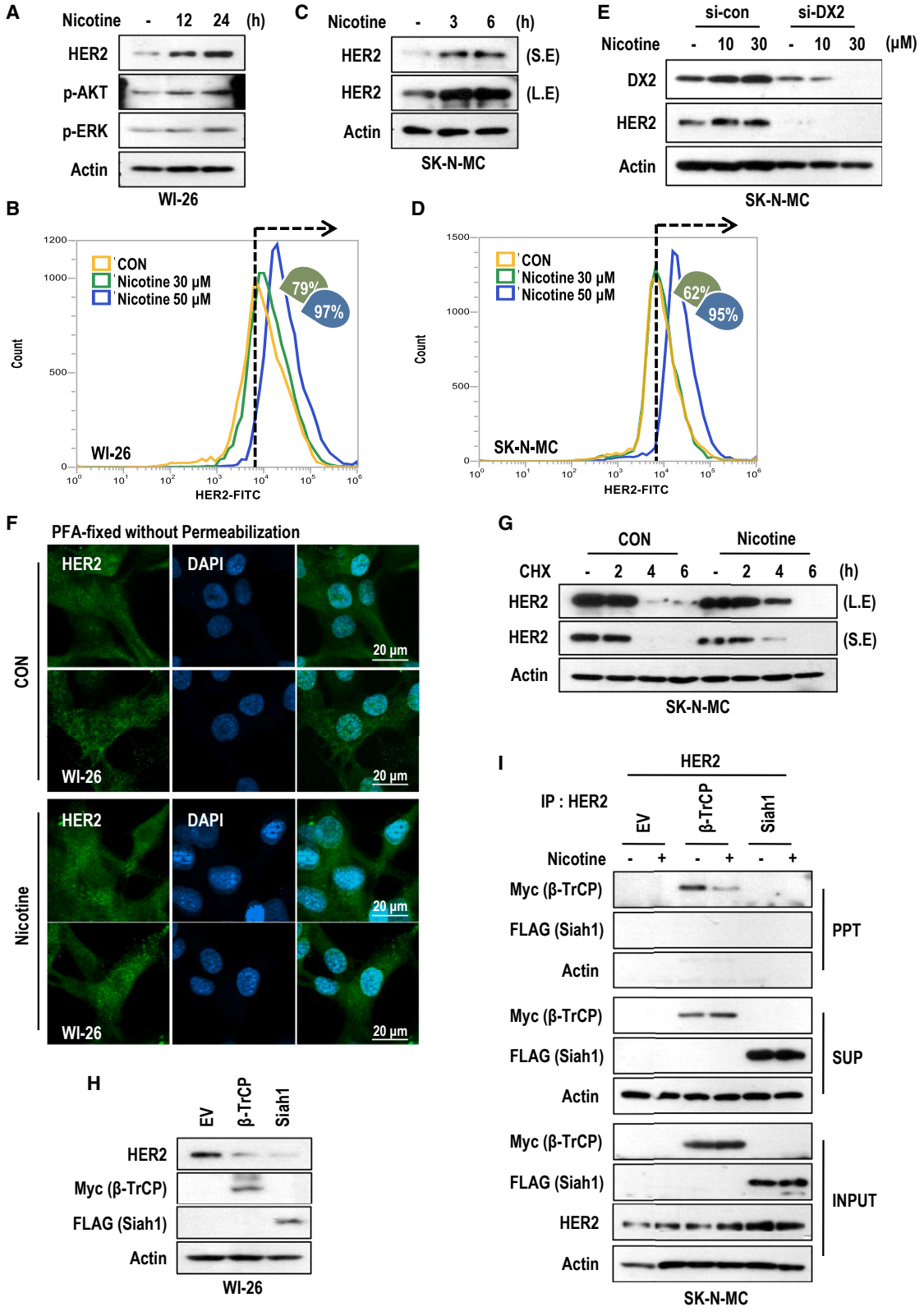

(legend on next page)

increased the DX2-HER2 interaction (Figure S4G). Collectively, the stabilization of DX2 by nicotine may be associated with HER2 and block β-TrCP-mediated HER2 degradation, resulting in HER2 activation. These results indicate that nicotine-induced DX2 expression contributes to cancer progression through HER2-mediated oncogenic signaling.

Nicotine activates Shh signaling

As shown in a previous study, the subcellular localization of DX2 was determined by p14/ARF.[15] DX2 localized in the nucleus and nucleolus in p14/ARF-intact cell lines (WI-26 and H1299; Figures S5A and S5B) and in the cytoplasm in p14/ARF-null cell lines (A549 and H460; Figures S5C and S5D). Also, the knockdown of p14/ARF induced the translocation of DX2 from the nucleus to the cytoplasm (Figures 3A and 3B). As more than 90% of SCLC has inactivating mutations of TP53, p14/ARF and DX2 may conduct another role at the nucleus in SCLC.[5,25] Besides, HER2 activation is well established in the progression of NSCLC but not critical in SCLC. In fact, SCLC cell lines did not express HER2 (Figure S5E). Considering our and other's previous studies that DX2 transgenic mice bear SCLC as well as NSCLC[15] and that smoking is a critical risk factor for SCLC,[3] nicotine would also be critically involved in SCLC. To address this, we first checked the expression of Shh, which has been shown to be elevated and secreted in SCLC without detailed molecular mechanisms[26] and regulated by p14/ARF.[27] As expected, nicotine induced Shh expression in WI-26 cells in a dose-dependent manner (Figure 3C). In SCLC cell lines, nicotine also increased Shh levels (Figures 3D and 3E) within 1 h. Since SCLC is known to be derived from neuroendocrine cells,[5] we monitored the effect of nicotine in SK-N-MC neuronal cells and found that Shh was induced at the transcriptional level by nicotine treatment (Figure S5F). Ectopic expression of DX2 also increased Shh expression (Figure 3F), whereas the elimination of DX2 by small interfering RNA (siRNA) abolished nicotine-induced Shh expression (Figures 3G, S5G, and S5H), indicating that DX2 was essential for nicotine-mediated Shh induction. The DX2 inhibitor[15] reduced Shh expression in SCLC (Figure 3H) and SK-N-MC (Figure S5I). To examine the role of elevated Shh by nicotine, we collected conditioned medium from nicotine-treated neuronal cells and treated them with WI-26 (Figure 3I). The conditioned media of SK-N-MC (Figure 3J) and SK-N-SH (Figure S5J) induced cyclin D1 expression in WI-26 cells. These results suggest that Shh released by nicotine-exposed cells might promote cell proliferation and may be an important feature for nicotine-induced tumorigenesis. To eliminate the effect of the nicotine that remained in the medium, we treated the conditioned medium with UV. Even after treatment with UV, the conditioned medium induced cyclin D1 expression (Figure S5K). Therefore, it is assumed that secreted Shh, not remaining nicotine, affects the proliferation of the surrounding cells.

Nicotine promotes tumorigenesis via DX2 induction

Next, we checked tumor sphere formation to obtain more direct evidence of nicotine and carcinogenesis. WI-26 cells were grown in suspension without attachment with or without nicotine. In contrast to the small spheroids in the control group, nicotine enhanced spheroid formation in a dose-dependent manner (Figure S6A). We observed clearer features after staining with phalloidin (Figure 4A). Compared with the control, the 30 μM nicotine-treated cells formed enlarged spheroids (Figure 4B). In these spheroids, we observed the induction of DX2, Shh, and HER2 (Figure 4C). To determine the relationship between spheroid formation and DX2 expression, we performed a spheroid formation assay in DX2-transfected and DX2-eliminated WI-26 cells. DX2-transfected cells could easily form spheroids regardless of nicotine treatment (Figure S6B). In contrast, DX2-deficient cells could not form spheroids, even under nicotine-treated conditions (Figures 4D and 4E). In fact, the elimination of DX2 completely blocked tumor sphere formation (Figures 4F and 4G). These results suggest that DX2 is critical for nicotine-induced tumorigenesis. To confirm the tumorigenic ability of nicotine *in vivo*, we administered nicotine intraperitoneally (i.p.) to wild-type mice (Figure S7A). Compared to the vehicle-treated group, the nicotine group developed Ki-67-positive highly proliferative tumors in lung (Figure 4H). Additionally, nicotine induces clear cell renal cell carcinoma (CCRCC) in another major nicotine-affected organ, the kidney (Figures S7C and S7D). Therefore, nicotine itself appears to have oncogenic capacity, which occurs through DX2.

Optimization of DX2 inhibitor

Since DX2 is essential for nicotine-induced tumorigenesis, an inhibitor of DX2 would be useful as an anti-cancer drug. Through ELISA-based chemical screening, we found a promising DX2

Figure 2. Induction of HER2 by nicotine in a DX2-dependent manner

(A) Expression of HER2 is induced by nicotine. WI-26 cells were treated with nicotine at 30 μM for the indicated time, and immunoblot was performed. Actin was used as a loading control. (B) Cell surface HER2 expression is elevated by nicotine. WI-26 cells were treated with nicotine at 30 μM for 6 h. Subsequently, PFA fixing was conducted without permeabilization. Then, cell surface HER2 expression was measured using flow cytometry. (C) Nicotine induces HER2 expression in SK-N-MC cells. Cells were treated with nicotine at 30 μM for the indicated time, and immunoblot was performed. Actin was used as a loading control. L.E and S.E indicate long exposure and short exposure, respectively. (D) Cell surface HER2 expression is elevated by nicotine. SK-N-MC cells were treated with nicotine at 30 μM for 6 h. (E) Knockdown of DX2 blocks nicotine-mediated HER2 induction. SK-N-MC cells were transiently transfected with control siRNA or DX2-specific siRNA. After 48 h, nicotine was treated. Expression of DX2 and HER2 was measured by western blot, and actin was used as a loading control. (F) Nicotine induces cell surface HER2 expression. Cells were treated with nicotine at 30 μM for 6 h. Subsequently, PFA fixing was conducted without permeabilization. For immunofluorescence (IF) assay, cells were stained with HER2 antibody, and DAPI was used for nuclei staining. Scale bar, 20 μm. (G) Half-life of HER2 is prolonged by nicotine. After being incubated with nicotine at 30 μM for 6 h, CHX was treated for the indicated time. Then, immunoblot analysis was performed. Actin was used as a loading control. L.E and S.E indicate long exposure and short exposure, respectively. (H) β-TrCP reduces HER2 expression. WI-26 cells were transiently transfected with β-TrCP and Siah1. Expression of HER2 was measured by western blot, and actin was used as a loading control. (I) Nicotine inhibits the interaction of HER2 and β-TrCP. To detect the interaction HER2 and β-TrCP, an immunoprecipitation (IP) assay was conducted using HER2 antibody. PPT indicates proteins that co-precipitate with HER2, and SUP indicates the supernatant.

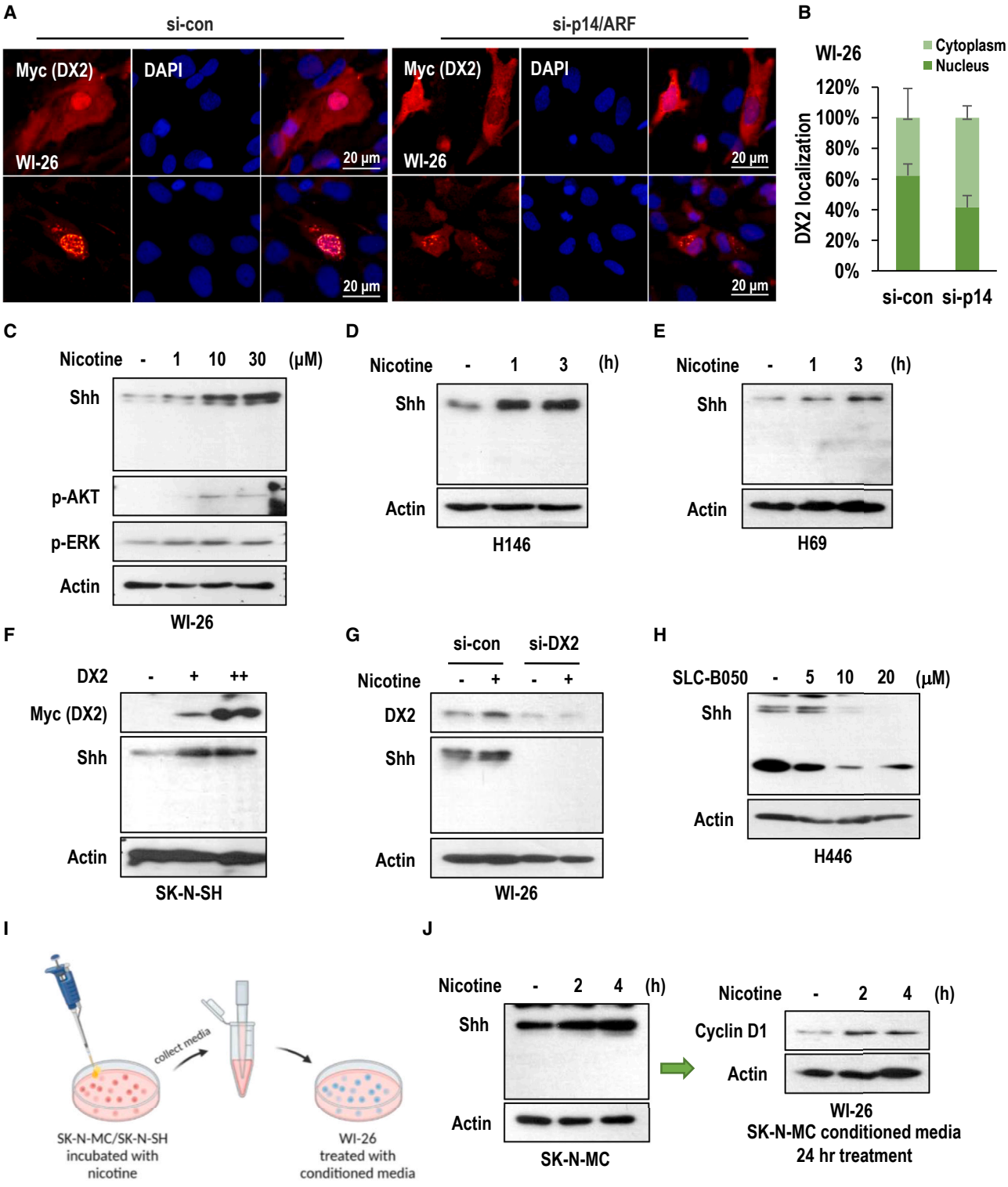

Figure 3. Activation of hedgehog signaling via induction of Shh expression

(A) In p14/ARF knockdown conditions, DX2 translocates to cytoplasm. WI-26 cells were transiently transfected with control siRNA or p14/ARF-specific siRNA. After 24 h, Myc-tagged vector encoding wild-type DX2 was transfected to WI-26 cells. For immunofluorescence (IF) assay, cells were stained with anti-Myc antibody, and DAPI was used for nuclei staining. Scale bar, 20 μm. (B) The intensity of rhodamine signal in nucleus or cytoplasm was measured and visualized. Error bars indicate the standard

(legend continued on next page)

inhibitor, SLC-B050, in our previous study.[15] However, because SLC-B050 has a very high half maximal inhibitory concentration (IC_{50}) value (>20 μM), chemical optimization is required. To identify a more effective candidate chemical, we generated 15 derivatives and examined their effect on DX2 expression. Compared to SLC-B050, 3 kinds of chemicals (SNU-10, -11, and −14) reduced DX2 expression more effectively (Figure 5A). SNU-14 clearly reduced DX2 expression at 2 μM (Figure S8A). The IC_{50} of SNU-14, based on a 3-(4,5-dimethythiazol-2-yl)-2,5-diphenyl tetrazolium bromide (MTT) assay, was less than 10 μM (Figure 5B). In contrast to the incomplete inhibition of SLC-B050 (Figure S8B), SNU-14 completely blocked nicotine-induced cell proliferation at a concentration of 5 μM (Figure S8C). Next, we examined the effects of SNU-14 on SCLC cell lines. In H446 cells, 1 μM SNU-14 seemed to be sufficient to reduce DX2 expression (Figure 5C). In addition, SNU-14 showed a very low IC_{50} in the MTT assay after 96 h (approximately 1–2 μM; Figure S8D). To obtain further evidence, we monitored the effect of SNU-14 on H146, another SCLC cell line. From the MTT assay, we found that 2 μM SNU-14 was sufficient to eliminate these cancer cells (Figures 5D and 5E). SNU-14 was even more effective at suppressing HER2 expression (Figure S8A) and Shh (Figures S8E and S8F) than SLC-B050. However, SNU-14 and SLC-B050 did not alter the viability of the normal fibroblasts (Figure 5F). This result implied that SNU-14 did not cause severe adverse effects when applied to cancer drugs.

Anti-tumoral effect of SNU-14

To confirm the anti-tumor effect of SNU-14, we treated it with nicotine-induced spheroids. Compared to SLC-B050, spheroids were diminished in the SNU-14-treated group (Figure 6A). Indeed, the size and number of spheroids were clearly reduced in the SNU-14-treated group (Figures 6B and 6C). Next, we examined the effect of our chemicals on nicotine-induced HER2 expression. The increased HER2 expression was inhibited by chemical treatment (Figures 6D and 6E). Considering our results, the inhibition of DX2 by chemicals could block nicotine-mediated tumorigenesis (Figure 6F).

DISCUSSION

Smoking is a well-documented risk factor for lung cancer.[3] Indeed, a reduction in the smoking rate can pull down the death rate of lung cancer.[28] Despite well-known epidemiological facts, the ultimate carcinogen in smoking has not been clearly suggested. Although tars and benzo-(a)-pyrene have been suggested as carcinogens in smoking, they have not fully elucidated smoking-related cancer formation because smoking is also closely associated with kidney and bladder cancer.[8–10,29] Therefore, water-soluble and circulating factors are related to smoking-related cancers. In this study, we demonstrated that nicotine is an important factor in smoking-related human cancers. Nicotine can induce DX2 (Figure 1A), an alternative splicing product of AIMP2 and an inhibitor of p14/ARF.[15] Nicotine-induced cell proliferation was completely blocked by the DX2 inhibitor (Figure S8B), suggesting that the tumorigenic potential of nicotine can be achieved by DX2 induction. In particular, the administration of nicotine induces lung and kidney cancer in wild-type mice. Therefore, we confirmed that nicotine acts as an ultimate carcinogen.

Nicotine can stabilize DX2 via a Ca^{2+}-mediated signaling cascade. Although we could not clearly demonstrate the signaling components, phosphorylation of the QDY motif, which is newly generated by alternative splicing, would be important for nicotine-mediated DX2 stabilization (Figure S3). Since Src has been proposed as a responsible kinase, a more intensive study will pinpoint a protein for DX2 stabilization and phosphorylation.

In this study, we also showed evidence that nicotine induced HER2 expression (Figures 2A–2D). HER2 is stabilized by DX2, which is suppressed by β-TrCP-mediated proteasomal degradation (Figures 2G–2I). Although HER2 is frequently amplified in NSCLC, a considerable proportion of patients with NSCLC show higher protein expression levels without genetic alternation.[19–21] Our findings provide a molecular basis for these patients. Although we did not perform a comparative analysis of HER2 expression between smokers and nonsmokers, it would be useful for understanding smoking-induced cancer progression. In addition, we observed Shh induction in response to nicotine. Shh has been suggested to be associated with SCLC and glioblastoma.[30–32] Considering that SCLC has been suggested to originate from neuroendocrine cells, the connection between SCLC and Shh seems to be reasonable. Indeed, Shh induced by nicotine promoted neighbor cell proliferation (Figure 3J).

Considering these results, nicotine may contribute to NSCLC and SCLC through the induction of HER2 and Shh (Figure 6F). Indeed, smoking is a risk factor for both NSCLC and SCLC. Furthermore, SCLC sometimes displays mixed features with NSCLC, a condition known as combined SCLC (C-SCLC), and approximately 20% of patients with SCLC have C-SCLC.[33,34] In addition, HER2 and Shh were induced by DX2 stabilization. The elimination of DX2 completely

deviations (SD). (C) Nicotine induces Shh expression in WI-26 cells. Cells were treated with nicotine of the indicated concentration for 24 h. Then, immunoblot or RT-PCT analysis was performed. Actin and GAPDH were used as loading controls. (D and E) Nicotine induces Shh expression in SCLC cells (H146 and H69). Cells were treated with nicotine at 30 μM for the indicated time. Then, immunoblot or RT-PCT analysis was performed. Actin and GAPDH were used as loading controls. (F) Exogenous expression of DX2 induces Shh. SK-N-SH cells were transiently transfected by Myc-tagged vector encoding DX2. After 24 h, immunoblot was conducted. Actin was used as a loading control. (G) Nicotine-mediated Shh induction is blocked by elimination of DX2 using siRNA. WI-26 cells were transiently transfected with control siRNA or DX2-specific siRNA. After 48 h, nicotine was treated for 24 h. Then, immunoblot was conducted, and actin was used as a loading control. (H) DX2 inhibitor reduces Shh expression. H446 cells were treated with SLC-B050 for 24 h. Subsequently, immunoblot was conducted. Actin was used as a loading control. (I) Diagram summarizing the experiment. Nicotine treatment was given to neuronal cells (SK-N-MC). After incubation, the conditioned medium was collected and given to WI-26 cells as treatment. Then, WI-26 cells were incubated with conditioned medium for 24 h. (J) In nicotine-treated SK-N-MC cells, expression of Shh is induced. In conditioned-medium-treated cells, expression of cyclin D1 was elevated. SK-N-MC cells were treated with nicotine at 30 μM for the indicated time. Then, conditioned medium was collected and given to WI-26 cells as a treatment. After 24 h, immunoblot was conducted. Actin was used as a loading control.

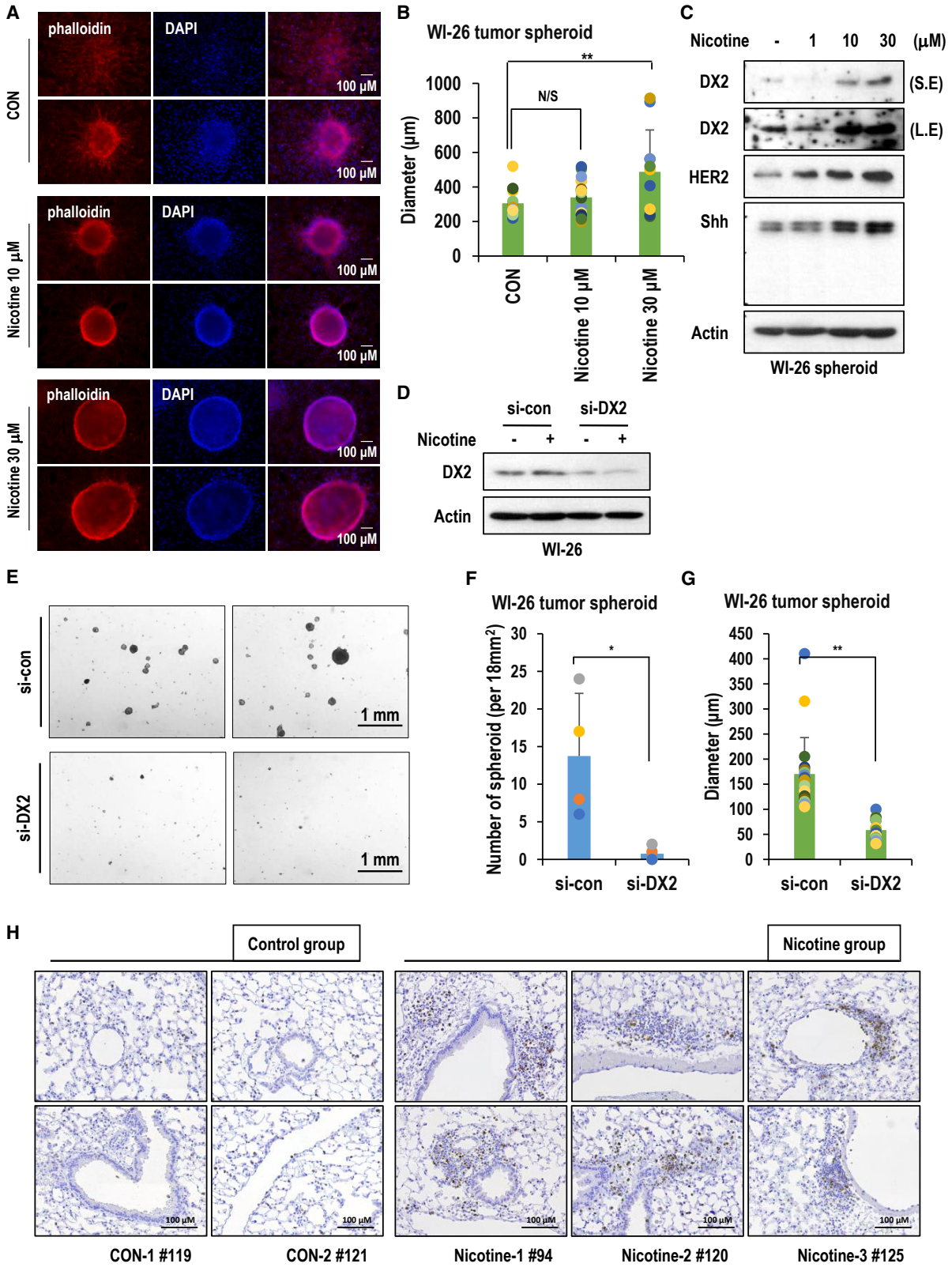

(legend on next page)

blocked HER2 and Shh expression (Figures 2E and 3G). Indeed, the newly generated strong DX2 inhibitor SNU-14 suppressed nicotine-induced tumor spheroid formation (Figure 4A) and SCLC cell viability (Figure 5). Although we have to test the effect of this chemical in animal models, the inhibition of DX2 by new chemicals would be a very promising strategy for smoking-related carcinogenesis (Figure 6F). Moreover, considering the safety of our chemical (Figure 5F), it would be useful for the prevention of smoking-related cancers, including bladder, kidney, and lung cancer.

MATERIALS AND METHODS

Cell culture and reagents

NSCLC cell lines (A549, H1299, and H460) and an SCLC cell line (NCI-H446) were obtained from the American Type Culture Collection (ATCC; Manassas, VA, USA) and maintained in RPMI-1640 or DMEM containing 10% fetal bovine serum (FBS) and 1% antibiotics. Human embryonic kidney (HEK293), human diploid lung fibroblast (WI-26), neuroblastoma (SK-N-SH and SK-N-MC), bladder carcinoma (253 J), and SCLC (NCI-H146, NCI-H128, NCI-H209, and NCI-H82) cell lines were purchased from the Korean Cell Line Bank (KCLB; Seoul, South Korea). SK-N-SH cells were maintained in minimal essential medium (MEM) containing 10% FBS, 1% antibiotics, 25 mM HEPES, and 300 mg/L L-Glu. HEK293, WI-26, SK-N-MC, and 253 J cells were cultured in DMEM containing 10% FBS and 1% penicillin-streptomycin. SCLC cells were maintained in RPMI-1640 medium containing 10% FBS and 1% antibiotics. The unaffected control (GM00038, 9-year-old female, N9) was obtained from Coriell Cell Repositories (Camden, NJ, USA) and maintained in Eagle's MEM (EMEM) supplemented with 15% FBS and 2 mM glutamine without antibiotics. The cell lines were maintained at 37°C with 5% CO_2 and certified by short tandem repeat analysis. Nicotine, BAPTA, and cycloheximide were purchased from Sigma-Aldrich (St. Louis, MO, USA). Actinomycin D, ALLN, MG132, PP2, and MTT were obtained from Calbiochem (Darmstadt, Germany).

Transfection of mammalian expression plasmids and siRNA

The Myc-fused AIMP2/p38 and DX2 vectors were obtained from Dr. Kim (Seoul National University, Seoul, Republic of Korea). The FLAG-tagged Siah-1 vector was provided by Dr. Lashuel (Qatar Foundation, Doha, Qatar). HER2/Neu and Myc-fused β-TrCP vectors were obtained from Addgene (Cambridge, MA, USA). Transfection was performed for 24 h using jetPEI (Polyplus Transfection, Illkirch, France) or Viafect reagent (Promega, Madison, WI, USA) according to the manufacturer's protocol. Briefly, the vectors were mixed with jetPEI in 150 mM NaCl solution or Viafect reagent in serum-free medium. After incubation, the mixtures were added to cells and incubated for 24 h. For *in vitro* gene knockdown, siRNAs against target proteins, including DX2, were generated by a custom service (Cosmo Genetech, Seoul, Republic of Korea). The sequences of si-DX2 were 5′-CTGGCCACGTGCAGGATTA-3′ (#1) and 5′-GCTGTCAACGCAACCCTTA-3′ (#3). The INTERFERin reagent (Polyplus Transfection) was used for siRNA transfection according to the manufacturer's protocol.

Chemical synthesis

The compounds used in chemical screenings were synthesized by Dr. Kwon (Seoul National University). The derivatives were developed based on the core parent structure of SLC-B050.

Immunoblot analysis

Proteins were extracted using radioimmunoprecipitation assay (RIPA) buffer (50 mmol/L Tris-Cl, 150 mmol/L NaCl, 1% NP-40, 0.1% SDS, and 10% sodium deoxycholate) and inactivated with sample buffer (heated at 95°C for 7 min). Protein samples were subjected to sodium dodecyl sulfate-polyacrylamide gel electrophoresis (SDS-PAGE) and transferred to polyvinylidene difluoride (PVDF) membranes. The membranes were blocked with 3% skim milk, 1% bovine serum albumin (BSA), or 0.1% gelatin from cold water fish skin for 1 h and incubated with specific primary antibodies for 2 h. The membranes were washed thrice and incubated with horseradish peroxidase (HRP)-conjugated goat anti-mouse or goat anti-rabbit secondary antibodies for 1 h at room temperature (RT). Protein bands were detected by chemiluminescence with an ECL kit (iNtRON Biotechnology, Gyeonggi-do, Korea). The following antibodies were used in this study: HER2 (1:1,000; 2165s; Cell Signaling Technology, Danvers, MA, USA), cyclin D1 (1:1,000; 2978s; Cell Signaling Technology), *p*-ERK (1:3,000; 4377s; Cell Signaling Technology), *p*-AKT (1:1,000, 4051s, Cell Signaling Technology), Actin (1:5,000; 66009-1-Ig; Proteintech, Chicago, IL, USA), Gli1 (1:3,000, 66905-1-Ig, Proteintech), Shh (1:10,000; ab53281; Abcam, Cambridge, UK), FLAG (1:1,000; F3105; Sigma-Aldrich), c-Myc (1:1,000; M5546; Sigma-Aldrich), and DX2 (1:10,000; HPAB-M0004-YC; Creative Biolabs, Shirley, NY, USA).

Protein-protein interaction analysis

Co-immunoprecipitation (coIP) assays were performed to analyze protein-protein interactions. For endogenous IP assays, whole-cell

Figure 4. Enhancement of tumor spheroid formation by nicotine

(A) Nicotine facilitates tumor spheroid formation. WI-26 cells were seeded in a non-coated cell plate and treated with nicotine for 7 days. Then, an IF assay was conducted to observe the spheroid. Phalloidin and DAPI were used for actin filaments and nuclei staining. Scale bar, 100 μm. (B) Based on Figure S6A, the diameter of spheroid was measured. $^{**}p < 0.005$. Error bars indicate the standard deviations (SD). (C) In nicotine-treated tumor spheroids, DX2, HER2, and Shh expression is elevated. Nicotine treatment was given to WI-26 spheroids for 3 weeks. Subsequently, immunoblot was performed. Actin was used as a loading control. L.E and S.E indicate long exposure and short exposure, respectively. (D and E) Nicotine-mediated tumor spheroid formation is blocked by elimination of DX2. WI-26 cells were transiently transfected with control siRNA or DX2-specific siRNA. After 48 h, cells were transported to a non-coated cell plate and treated with nicotine. After incubation for 3 days, tumor spheroid formation was monitored using a microscope. Scale bar, 1 mm. (F and G) Knockdown of DX2 blocks nicotine-mediated tumor spheroid formation. Based on Figure 4E, the number of spheroids and diameter of spheroids was measured. $^{**}p < 0.005$. N.S. indicates no significance. Error bars indicate the standard deviations (SD). (H) Immunohistochemical staining of Ki-67 expression in lung. Compared to vehicle-treated mice, tumor regions were detected in nicotine-treated mice ($n = 3$). 20×. Scale bar, 100 μm.

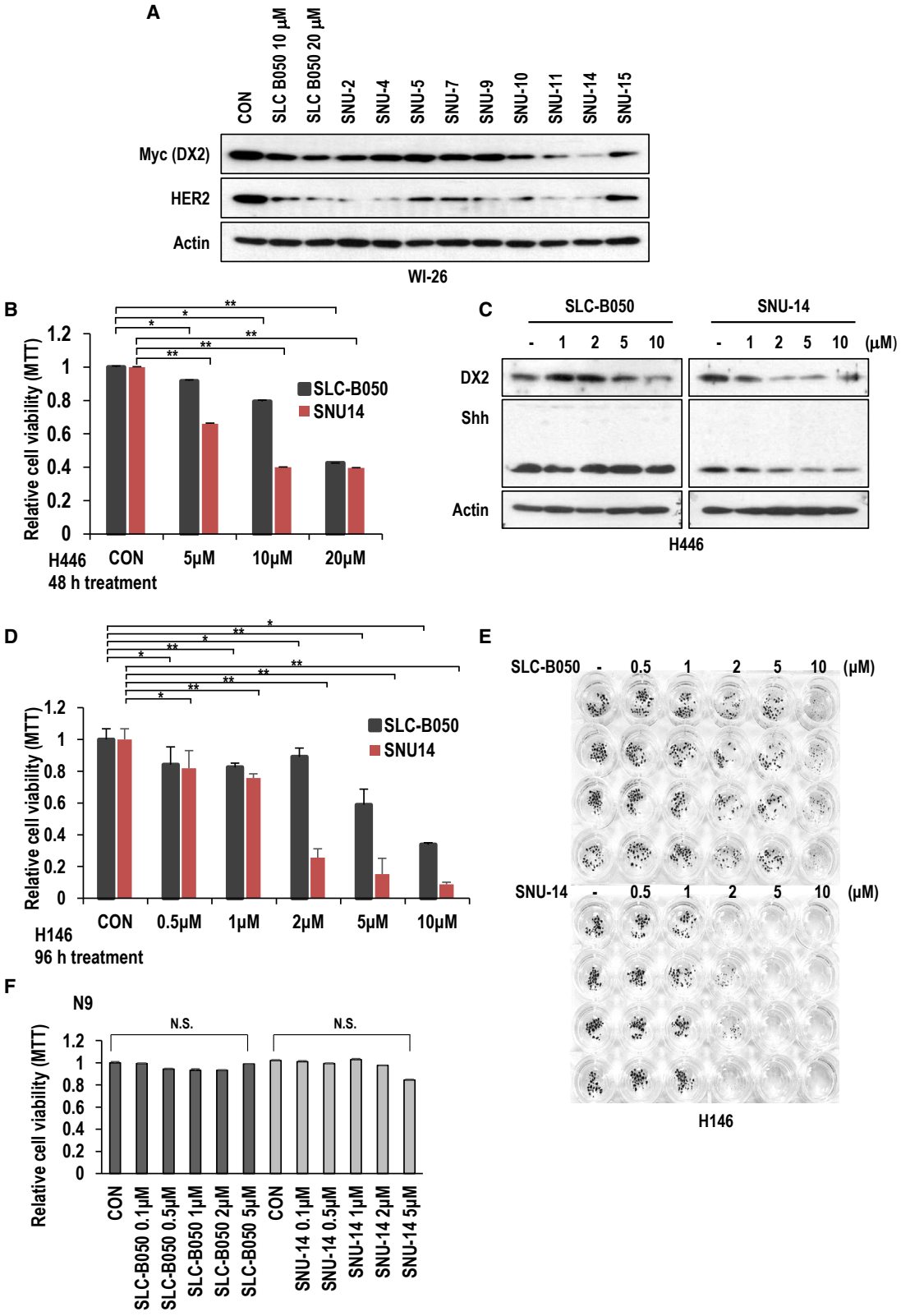

(legend on next page)

lysates were incubated with anti-HER2 or anti-Myc antibody at 4°C overnight, followed by incubation with protein A/G-conjugated agarose beads (Invitrogen, Waltham, MA, USA) at 4°C for 1 h. After centrifugation and washing with phosphate-buffered saline (PBS), the precipitated proteins were detected by SDS-PAGE and immunoblotting with antibodies that bind the putative associated proteins.

IF staining

Cells were cultured on coverslips, transfected with the indicated vectors, or treated with the indicated chemicals. Cells on coverslips were fixed with 1% paraformaldehyde (PFA) for 1 h at RT and then permeabilized with 0.1% Triton X-100/PBS for 5 min. After blocking with goat serum solution (diluted 1:400 in PBS) for 1 h, cells were incubated with specific primary antibodies in blocking solution overnight at 4°C. Then, the cells were incubated with fluorescein isothiocyanate (FITC) and/or rhodamine-conjugated secondary antibodies at 4°C for 8 h. Nuclei were stained with DAPI (4, 6-diamidino-2-phenylindole) at RT for 10 min. After washing with PBS, coverslips were mounted with mounting solution (H-5501; Vector Laboratories, Burlingame, CA, USA) and analyzed using a fluorescence microscope (CELENA S, Logos Biosystems, Gyeonggi-do, Korea). The following antibodies were used for IF staining: HER2 (1:200) and anti-c-Myc (1:400). To detect cell surface HER2, an IF assay was performed without permeabilization. To obtain tumor spheroid IF images, spheroids in uncoated dishes were transferred onto coverslips and fixed. After staining with DAPI and phalloidin, the spheroids were monitored using fluorescence microscopy (CELENA X, Logos Biosystems). z stack images were acquired, and multiple focal planes were merged.

RNA isolation and RT-PCR

For reverse transcription polymerase chain reaction (RT-PCR), total cellular RNA was extracted using an RNA extraction kit (Qiagen, Hilden, Germany). Using M-MLV (Moloney murine leukemia virus) reverse transcriptase (Invitrogen) and random hexamers, 1 μg of total RNA was reverse transcribed to cDNA. Gene expression studies were performed using the following primers.

h*DX2* (forward): 5′-TACCTGGACCTCCCGAAGTGC-3′

h*DX2* (reverse): 5′-GGAGAGGCCATCAACTGCAGC-3′

h*HER2* (forward): 5′-GTGTGGACCTGGATGACAAGG-3′

h*HER2* (reverse): 5′-GCTCCACCAGCTCCGTTTCCTG-3′

h*SHH* (forward): 5′-CCCTTTAGCCTACAAGCAGT-3′

h*SHH* (reverse): 5′-CCACTGGTTCATCACAGAG-3′

h*GAPDH* (forward): 5′-ATCTTCCAGGAGCGAGATCCC-3′

h*GAPDH* (reverse): 5′-AGTGAGCTTCCCGTTCAGCTC-3′

Measurement of cell viability

The cells were treated with varying concentrations of the drug for the indicated durations. To determine the cellular viability, cells were incubated with 0.5 mg/mL of MTT solution (475989; Merck, Darmstadt, Germany) for 4 h at 37°C. After removing the supernatant, the precipitate was dissolved in 200 μL DMSO and quantified by measuring the absorbance at 540 nm. After incubation with the indicated chemicals, cell proliferation was measured by live-cell time-lapse imaging (Incucyte Live-Cell Analysis Systems, Sartorius, Göttingen, Germany).

Flow cytometry analysis

Flow cytometry was performed to detect HER2 expression on the cell surface. After incubation with nicotine, the cells were suspended in EDTA. Then, the cells were fixed with 1% PFA without permeabilization and stained with HER2 antibody. After washing, FITC-conjugated secondary antibodies were added, and the FITC signal of each cell was measured by flow cytometry (Attune NxT Acoustic Flow Cytometer, Thermo Fisher Scientific, Waltham, MA, USA).

Tumor spheroid-forming assay

The cells were cultured in a non-coated cell plate and treated with the indicated chemicals. Under floating conditions, cells with the ability to transform gradually generated cell aggregates and eventually produced tumor spheroids. The diameters of the spheroids were measured using a CELENA X Imaging System.

In vivo experiment

Animal experiments were performed in a facility certified by the Association for Assessment and Accreditation of Laboratory Animal Care in compliance with animal policies approved by Pusan National University. All mice were maintained under temperature- and

Figure 5. Improved effect of SLC-B050 derivatives

(A) Some SLC-B050 derivatives inhibit the expression of DX2 and HER2 more effectively at the same concentration. WI-26 cells were transiently transfected by Myc-tagged vector encoding DX2. After 24 h, SLC-B050 and its derivatives were treated at 10 or 20 μM for 24 h. Subsequently, immunoblot was performed. Actin was used as a loading control. (B) SNU-14 more effectively inhibits H446 cell viability than SLC-B050. H446 cells were treated with SLC-B050 or SNU-14 of the indicated concentration for 48 h. Then, cell viability was measured by MTT assay. *$0.005 < p < 0.05$ and **$p < 0.005$. Error bars indicate the standard deviations (SD). (C) SNU-14 reduces DX2 expression more effectively than SLC0B050 in H446 cells. Cells were treated with SLC-B050 and SNU-14 of the indicated concentration for 12 h. Subsequently, immunoblot was performed. Actin was used as a loading control. (D) Cell viability measured by MTT assay indicates that SNU-14 was more effective than SLC-B050 for SCLC treatment. After treatment with chemicals of the indicated concentration for 96 h in serum-containing conditions, cell viability was measured by MTT assay ($n = 4$ independent experiment; two-tailed Student's t test). *$0.005 < p < 0.05$ and **$p < 0.005$. Error bars indicate the standard deviations (SD). (E) Cell death of H146 occurred more excessively with SNU-14. After treated with chemicals of the indicated concentration for 96 h, using MTT solution, formazan crystal was observed ($n = 4$ independent experiment; two-tailed Student's t test). (F) Both SLC-B050 and SNU-14 do not show cytotoxicity to normal fibroblasts. Cells were treated with SLC-B050 and SNU-14 of the indicated concentration for 48 h. Then, cell viability was measured by MTT assay ($n = 3$ independent experiment; two-tailed Student's t test). **$p < 0.005$. N.S. indicates no significance.

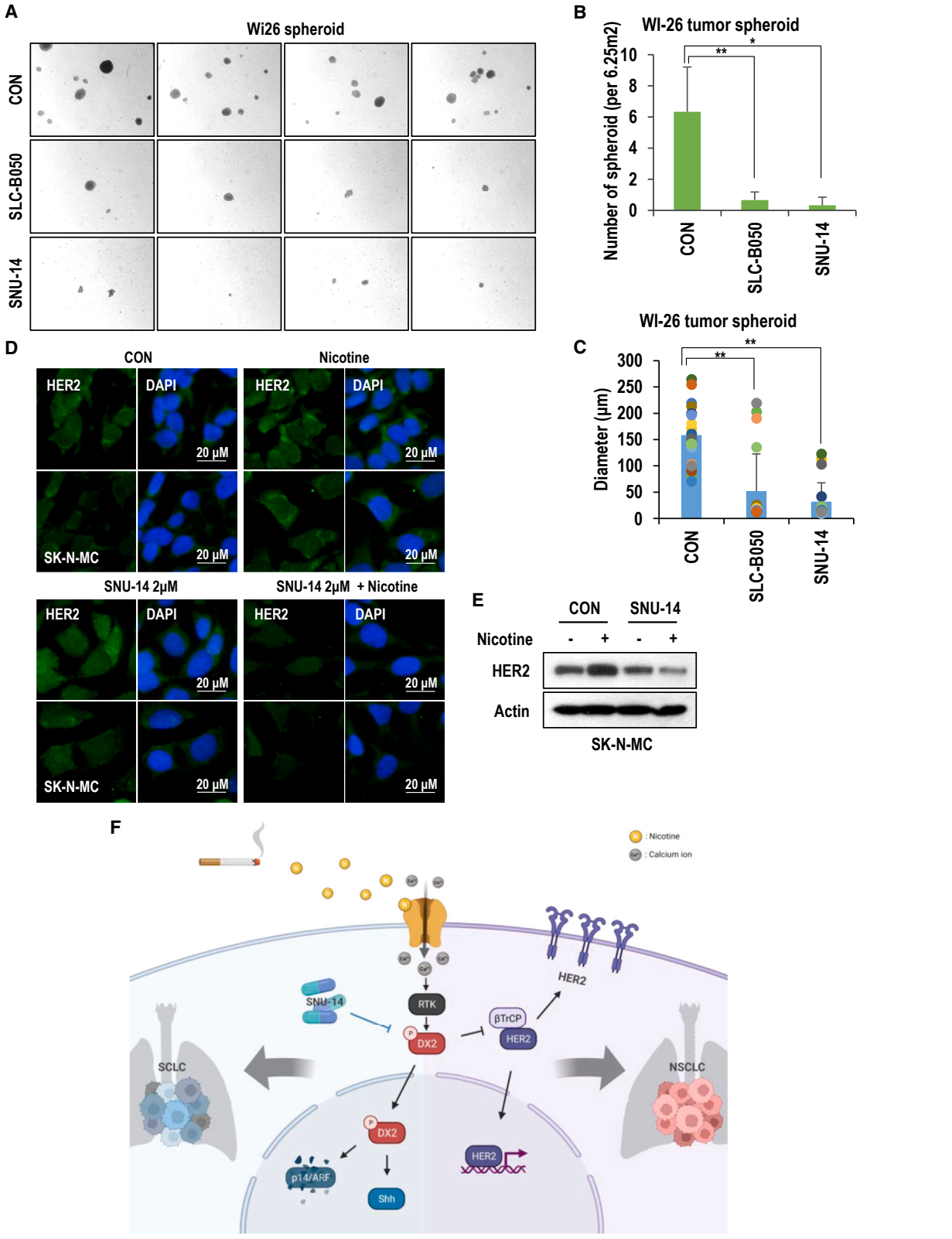

(legend on next page)

light-controlled conditions (20°C–23°C, 12/12 h light/dark cycle) and provided with autoclaved food and water. Wild-type mice (C57BL/6) were administered an i.p. injection of vehicle (PBS; $n = 3$) or nicotine (0.5 mg/kg, $n = 4$), three times per week for 12 weeks.

For histology analysis, lung and kidney tissues were fixed using 4% PFA for 48 h and embedded in paraffin blocks according to a basic tissue processing procedure. After deparaffinization and rehydration, hematoxylin and eosin (H&E) staining or immunohistochemistry (IHC) for Ki-67 was performed.

Statistical analysis

Data were analyzed using an unpaired or paired Student's t test. Statistical significance was set at $p < 0.05$. Error bars indicate standard deviation (SD). Data are expressed as the mean ± SD of at least two independent experiments.

DATA AND CODE AVAILABILITY

The data generated in this study are available within the article and its supplemental information file. All other data that support the findings of this study are available from the corresponding author upon reasonable request.

ACKNOWLEDGMENTS

This work was supported by National Research Foundation of Korea (NRF) grants funded by the Korean government (MSIT) (RS-2024-00399681 and RS-2024-00339289).

AUTHOR CONTRIBUTIONS

B.-J.P. handled the conceptualization and supervised the entire process. S.P. performed the experiments, analyzed the data, and drafted the manuscript. A.-Y.O., S.-m.K., T.-G.W., and B.-H.K. conceived the experimental designs and interpretation of data. B.-S.H. contributed to the *in vivo* experiments and analysis. Y.-J.S., H.J., H.S., and Y.K. synthesized and offered the chemicals. H.-P.P., J.J., and H.-J.K. performed the experiments.

DECLARATION OF INTERESTS

The authors declare no competing interests.

SUPPLEMENTAL INFORMATION

Supplemental information can be found online at https://doi.org/10.1016/j.omton.2024.200875.

REFERENCES

1. Sung, H., Ferlay, J., Siegel, R.L., Laversanne, M., Soerjomataram, I., Jemal, A., and Bray, F. (2021). Global cancer statistics 2020: GLOBOCAN estimates of incidence and mortality worldwide for 36 cancers in 185 countries. CA. Cancer J. Clin. *71*, 209–249.
2. Motadi, L.R., Misso, N.L., Dlamini, Z., and Bhoola, K.D. (2007). Molecular genetics and mechanisms of apoptosis in carcinomas of the lung and pleura: Therapeutic targets. Int. Immunopharmacol. *7*, 1934–1947.
3. Inamura, K. (2017). Lung cancer: understanding its molecular pathology and the 2015 WHO classification. Front. Oncol. *7*, 193.
4. Oronsky, B., Reid, T.R., Oronsky, A., and Carter, C.A. (2017). What's New in SCLC? A Review. Neoplasia *19*, 842–847.
5. Semenova, E.A., Nagel, R., and Berns, A. (2015). Origins, genetic landscape, and emerging therapies of small cell lung cancer. Genes Dev. *29*, 1447–1462.
6. Rudin, C.M., Brambilla, E., Faivre-Finn, C., and Sage, J. (2021). Small-cell lung cancer. Nat. Rev. Dis. Primers *7*, 3.
7. Hennings, H., Shores, R., Wenk, M.L., Spangler, E.F., Tarone, R., and Yuspa, S.H. (1983). Malignant conversion of mouse skin tumours is increased by tumour initiators and unaffected by tumour promoters. Nature *304*, 67–69.
8. Cinciripini, P.M., Hecht, S.S., Henningfield, J.E., Manley, M.W., and Kramer, B.S. (1997). Tobacco addiction: implications for treatment and cancer prevention. J. Natl. Cancer Inst. *89*, 1852–1867.
9. Hecht, S.S. (2003). Tobacco carcinogens, their biomarkers and tobacco-induced cancer. Nat. Rev. Cancer *3*, 733–744.
10. Narkowicz, S., Polkowska, Ż., Kiełbratowska, B., and Namieśnik, J. (2013). Environmental Tobacco Smoke: Exposure, Health Effects, and Analysis. Crit. Rev. Environ. Sci. Technol. *43*, 121–161.
11. DeMarini, D.M., Landi, S., Tian, D., Hanley, N.M., Li, X., Hu, F., Roop, B.C., Mass, M.J., Keohavong, P., Gao, W., et al. (2001). Lung tumor KRAS and TP53 mutations in nonsmokers reflect exposure to PAH-rich coal combustion emissions. Cancer Res. *61*, 6679–6681.
12. Kalet, B.T., Anglin, S.R., Handschy, A., O'Donoghue, L.E., Halsey, C., Chubb, L., Korch, C., and Duval, D.L. (2013). Transcription factor Ets1 cooperates with estrogen receptor α to stimulate estradiol-dependent growth in breast cancer cells and tumors. PLoS One *8*, e68815.
13. Benowitz, N.L., Hukkanen, J., and Jacob, P. (2009). Nicotine chemistry, metabolism, kinetics and biomarkers. Handb. Exp. Pharmacol. 29–60.
14. Govind, A.P., Vezina, P., and Green, W.N. (2009). Nicotine-induced upregulation of nicotinic receptors: Underlying mechanisms and relevance to nicotine addiction. Biochem. Pharmacol. *78*, 756–765.
15. Oh, A.Y., Jung, Y.S., Kim, J., Lee, J.H., Cho, J.H., Chun, H.Y., Park, S., Park, H., Lim, S., Ha, N.C., et al. (2016). Inhibiting DX2-p14/ARF interaction exerts antitumor effects in lung cancer and delays tumor progression. Cancer Res. *76*, 4791–4804.
16. Ratschiller, D., Heighway, J., Gugger, M., Kappeler, A., Pirnia, F., Schmid, R.A., Borner, M.M., and Betticher, D.C. (2003). Cyclin D1 overexpression in bronchial epithelia of patients with lung cancer is associated with smoking and predicts survival. J. Clin. Oncol. *21*, 2085–2093.
17. Zhong, C., Talmage, D.A., and Role, L.W. (2013). Nicotine elicits prolonged calcium signaling along ventral hippocampal axons. PLoS One *8*, e82719.

Figure 6. Improved anti-cancer effect of DX2 inhibitor

(A) Tumor spheroid formation is blocked by treatment of SLC-B050 and SNU-14. WI-26 cells were seeded to non-coated cell plate, and SLC-B050 or SNU-14 treatment at 10 μM was given to these cells. After incubation for 7 days, tumor spheroid formation was monitored using a microscope. (B) DX2 inhibitors effectively block tumor spheroid formation. Based on Figure 6A, the number of spheroids was counted. *$0.005 < p < 0.05$ and **$p < 0.005$. Error bars indicate the standard deviations (SD). (C) SNU-14 generates smaller tumor spheroids than SLC-B050. Based on Figure 31A, the diameter of the spheroid was measured. Error bars indicate the standard deviations (SD). (D) SNU-14 blocks nicotine-mediated HER2 induction. Cells were treated with SNU-14 at 2 μM and nicotine at 30 μM for 24 h. Then, immunoblot was conducted. Actin was used as a loading control. Scale bar, 20 μm. (E) SNU-14 reduces HER2 cell surface expression induced by nicotine. Cells were treated with SNU-14 at 2 μM and nicotine at 30 μM for 24 h. Cells were fixed with 4% PFA and incubated with HER2 antibody. DAPI was used for nuclei staining. (F) Summary diagram. DX2 is stabilized by nicotine, which is triggered by Src kinase through nAChR-mediated Ca^{2+} signaling. In the p14/ARF-intact state, DX2, stabilized by nicotine, transports to the nucleus. DX2 in the nucleus inhibits p14/ARF and activates Hh signaling. It results in cell death or proliferation of its own or surrounding cells and, consequently, promotes SCLC. In p14/ARF-null cells, DX2 exists in the cytoplasm and blocks the interaction of β-TrCP/HER2. Increased HER2 localizes on the cell surface or transports to the nucleus, probably to act as a transcription factor. Consequently, it causes NSCLC. The optimized DX2 inhibitor SNU-14 may inhibits the progression of lung cancer, particularly SCLC.

18. Kabbani, N., and Nichols, R.A. (2018). Beyond the channel: metabotropic signaling by nicotinic receptors. Trends Pharmacol. Sci. *39*, 354–366.

19. Hirsch, F.R., Varella-Garcia, M., Franklin, W.A., Veve, R., Chen, L., Helfrich, B., Zeng, C., Baron, A., and Bunn, P.A., Jr. (2002). Evaluation of HER-2/neu gene amplification and protein expression in non-small cell lung carcinomas. Br. J. Cancer *86*, 1449–1456.

20. Iqbal, N., and Iqbal, N. (2014). Human Epidermal Growth Factor Receptor 2 (HER2) in Cancers: Overexpression and Therapeutic Implications. Mol. Biol. Int. *2014*, 852748–852749.

21. Nakamura, H., Saji, H., Ogata, A., Hosaka, M., Hagiwara, M., Kawasaki, N., and Kato, H. (2003). Correlation between encoded protein overexpression and copy number of the HER2 gene with survival in non-small cell lung cancer. Int. J. Cancer *103*, 61–66.

22. Wang, Y.N., and Hung, M.C. (2012). Nuclear functions and subcellular trafficking mechanisms of the epidermal growth factor receptor family. Cell Biosci. *2*, 13.

23. Bi, Y., Gong, L., Liu, P., Xiong, X., and Zhao, Y. (2021). Nuclear ErbB2 represses DEPTOR transcription to inhibit autophagy in breast cancer cells. Cell Death Dis. *12*, 397.

24. Wang, H.M., Xu, Y.F., Ning, S.L., Yang, D.X., Li, Y., Du, Y.J., Yang, F., Zhang, Y., Liang, N., Yao, W., et al. (2014). The catalytic region and PEST domain of PTPN18 distinctly regulate the HER2 phosphorylation and ubiquitination barcodes. Cell Res. *24*, 1067–1090.

25. George, J., Lim, J.S., Jang, S.J., Cun, Y., Ozretić, L., Kong, G., Leenders, F., Lu, X., Fernández-Cuesta, L., Bosco, G., et al. (2015). Comprehensive genomic profiles of small cell lung cancer. Nature *524*, 47–53.

26. Velcheti, V., and Govindan, R. (2007). Hedgehog Signaling Pathway and Lung Cancer. J. Thorac. Oncol. *2*, 7–10.

27. Caserta, T.M., Kommagani, R., Yuan, Z., Robbins, D.J., Mercer, C.A., and Kadakia, M.P. (2006). p63 overexpression induces the expression of Sonic Hedgehog. Mol. Cancer Res. *4*, 759–768.

28. Thun, M.J., and Jemal, A. (2006). How much of the decrease in cancer death rates in the United States is attributable to reductions in tobacco smoking? Tob. Control *15*, 345–347.

29. Yuge, K., Kikuchi, E., Hagiwara, M., Yasumizu, Y., Tanaka, N., Kosaka, T., Miyajima, A., and Oya, M. (2015). Nicotine induces tumor growth and chemoresistance through activation of the PI3K/Akt/mTOR pathway in bladder cancer. Mol. Cancer Ther. *14*, 2112–2120.

30. Lim, S., Lim, S.M., Kim, M.J., Park, S.Y., and Kim, J.H. (2019). Sonic Hedgehog Pathway as the Prognostic Marker in Patients with Extensive Stage Small Cell Lung Cancer. Yonsei Med. J. *60*, 898–904.

31. Park, K.S., Martelotto, L.G., Peifer, M., Sos, M.L., Karnezis, A.N., Mahjoub, M.R., Bernard, K., Conklin, J.F., Szczepny, A., Yuan, J., et al. (2011). A crucial requirement for Hedgehog signaling in small cell lung cancer. Nat. Med. *17*, 1504–1508.

32. Watkins, D.N., Berman, D.M., and Baylin, S.B. (2003). Hedgehog Signaling: Progenitor Phenotype in Small-Cell Lung Cancer. Cell Cycle *2*, 196–198.

33. Wanger, P.L., Kitabayashi, N., Chen, Y., and Saqi, A. (2009). Combined Small Cell Lung Carcinomas: Genotypic and Immunophenotypic Analysis of the Separate Morphologic Components. Am. J. Clin. Pathol. *131*, 376–382.

34. Qin, J., and Lu, H. (2018). Combined small-cell lung carcinoma. OncoTargets Ther. *11*, 3505–3511.